

Supplementary Information

High-power Broadband Organic THz Generator

Jae-Hyeok Jeong^{†,1}, Bong-Joo Kang^{†,2}, Ji-Soo Kim¹, Mojca Jazbinsek³, Seung-Heon Lee¹, Seung-Chul Lee¹, In-Hyung Baek², Hoseop Yun⁴, Jongtaek Kim^{5,6}, Yoon Sup Lee⁵, Jae-Hyeok Lee¹, Jae-Ho Kim¹, Fabian Rotermund^{*,2}, and O-Pil Kwon^{*,1}

¹ Department of Molecular Science and Technology, Ajou University, Suwon 443-749, Korea

² Department of Physics & Division of Energy Systems Research, Ajou University, Suwon 443-749, Korea

³ Rainbow Photonics AG, Farbhofstrasse 21, CH-8048 Zurich, Switzerland

⁴ Department of Chemistry & Division of Energy Systems Research, Ajou University, Suwon 443-749, Korea

⁵ Department of Chemistry, Korea Advanced Institute of Science and Technology (KAIST), Daejeon 305-701, Korea

⁶ Department of Basic Science, Korea Air Force Academy, Cheongju 363-849, Korea

*Correspondence and requests for materials should be addressed to O.-P. K. (opilkwon@ajou.ac.kr) and F. R. (rotermun@ajou.ac.kr)

[†] equally contributed

Synthesis of HMQ-TMS

A. Synthesis by metathesis reaction

2-(4-Hydroxy-3-methoxystyryl)-1-methylquinolinium iodide (HMQ-I) (0.80 g, 1.92 mmol) was dissolved in methanol (650 mL). Silver(I) 2,4,6-trimethylbenzenesulfonate (0.59 g, 1.92 mmol, 1 equiv.) was dissolved in methanol (50 mL) and dropwised into the solution of HMQ-I. The precipitated AgI with white color was filtered off. The filtered solution was slightly evaporated and cooled down in freezer. Brown powder was then obtained. The final product was obtained by recrystallization in methanol and dried in vacuum oven at 60 °C overnight. Yield = 57 %. ¹H-NMR (400 MHz, CD₃OD, δ): 8.82 (d, 1H, *J* = 9.2, C₅H₂N), 8.43 (d, 1H, *J* = 9.2 Hz, C₆H₄), 8.39 (d, 1H, *J* = 8.8 Hz, C₅H₂N), 8.24 (d, 1H, *J* = 8.2 Hz, C₆H₄), 8.15 (m, 1H, C₆H₄), 8.06 (d, 1H, *J* = 15.6 Hz, CH), 7.90 (t, 1H, *J* = 7.4 Hz, C₆H₄), 7.67 (d, 1H, *J* = 16.0 Hz, CH), 7.52 (s, 1H, C₆H₃), 7.39 (d, 1H, C₆H₃), 6.91 (d, 1H, *J* = 8.0 Hz, C₆H₃), 6.83 (s, 2H, C₆H₂SO₃⁻), 4.56 (s, 3H, NCH₃), 3.98 (s, 3H, OCH₃), 2.60 (s, 6H, 2CH₃), 2.21 (s, 3H, CH₃).

B. Synthesis by condensation reaction

1,2-Dimethylquinolinium 2,4,6-trimethylbenzenesulfonate: 2-Methylquinoline (18.5 ml, 0.130 mol) and methyl 2,4,6-trimethylbenzenesulfonate (27.82 g, 0.130 mol, 1 equiv.) were dissolved in 1,2-dimethoxyethane and the solution was stirred at 70 °C for 4 days. The precipitated powder with white color was filtered and dried in vacuum oven at 50 °C overnight. Finally, we obtained light pink powder. Yield = 50 %. ¹H-NMR (400 MHz, CDCl₃, δ): 8.68 (d, 1H, *J* = 8.4, C₅H₂N), 8.42 (d, 1H, *J* = 8.8, C₆H₄), 8.11 (d, 1H, *J* = 8.0, C₆H₄), 8.10 (m, 1H, C₆H₄), 7.85 (d, 1H, *J* = 8.4, C₅H₂N), 7.84 (t, 1H, *J* = 7.8, C₆H₄), 6.65 (s, 2H, C₆H₂SO₃⁻), 4.69 (s, 3H, NCH₃), 3.26 (s, 3H, CH₃), 2.47 (s, 6H, 2CH₃), 2.16 (s, 3H, CH₃).

HMQ-TMS: HMQ-TMS was synthesized by condensation reaction with 1,2-dimethylquinolinium 2,4,6-trimethylbenzenesulfonate and vanillin, as in a similar manner with

HMQ-T [Kim, P.-J. *at al.* Highly efficient organic THz generator pumped at near-infrared: quinolinium single crystals. *Adv. Funct. Mater.* **22**, 200–209 (2012).]. Yield = 51 %. ¹H-NMR (400 MHz, CD₃OD, δ): 8.82 (d, 1H, *J* = 9.2, C₅H₂N), 8.43 (d, 1H, *J* = 9.2 Hz, C₆H₄), 8.39 (d, 1H, *J* = 8.8 Hz, C₅H₂N), 8.24 (d, 1H, *J* = 8.2 Hz, C₆H₄), 8.15 (m, 1H, C₆H₄), 8.06 (d, 1H, *J* = 15.6 Hz, CH), 7.90 (t, 1H, *J* = 7.4 Hz, C₆H₄), 7.67 (d, 1H, *J* = 16.0 Hz, CH), 7.52 (s, 1H, C₆H₃), 7.39 (d, 1H, C₆H₃), 6.91 (d, 1H, *J* = 8.0 Hz, C₆H₃), 6.83 (s, 2H, C₆H₂SO₃⁻), 4.56 (s, 3H, NCH₃), 3.98 (s, 3H, OCH₃), 2.60 (s, 6H, 2CH₃), 2.21 (s, 3H, CH₃). Elemental analysis for C₂₈H₂₉NO₅S: Calcd. C 68.41, H 5.94, N 2.85, S 6.52; Found C 68.48, H 5.87, N 2.89, S 6.38.

Quantum mechanical calculations

To investigate the macroscopic optical nonlinearities of HMQ-TMS crystals, we performed quantum mechanical calculation using finite field (FF) density functional theory (DFT) with B3LYP/6-311+G* considering molecular conformation and molecular ordering of HMQ cations in the crystal structure. The molecular conformation of HMQ-TMS(EXP) cation was obtained from the crystal structure of HMQ-TMS.

Table S1. Calculated results of the finite-field (FF) method with the experimental (EXP) cation structures of HMQ-TMS crystals at B3LYP/6-311+G(d) level: the zero-frequency hyperpolarizability tensor β_{ijk} ($\times 10^{-30}$ esu), the first-order hyperpolarizability β_{\max} ($\times 10^{-30}$ esu). The molecular conformation of HMQ-TMS(EXP) cation is obtained from the crystal structure of HMQ-TMS.

HMQ-TMS cation (EXP) ($\times 10^{-30}$ esu)	$\beta_{xxx} = 0.29$	$\beta_{xxy} = 0.13$	$\beta_{xyy} = 0.19$	$\beta_{yyy} = -0.74$	$\beta_{xxz} = 0.60$	$\beta_{xyz} = 0.48$
	$\beta_{yyz} = 8.28$	$\beta_{xzz} = 0.65$	$\beta_{yzz} = -39.05$	$\beta_{zzz} = 171.25$	$\beta_{\max} = 185$	

Table S2. The components of β_{ijk}^{eff} tensor ($\times 10^{-30}$ esu) in the Cartesian XYZ coordinate system.

HMQ-TMS ($\times 10^{-30}$ esu)	β_{333}^{eff}	β_{223}^{eff}	β_{113}^{eff}	β_{111}^{eff}	β_{221}^{eff}	β_{331}^{eff}
	184.6	0.7	-0.8	0.7	0.3	0

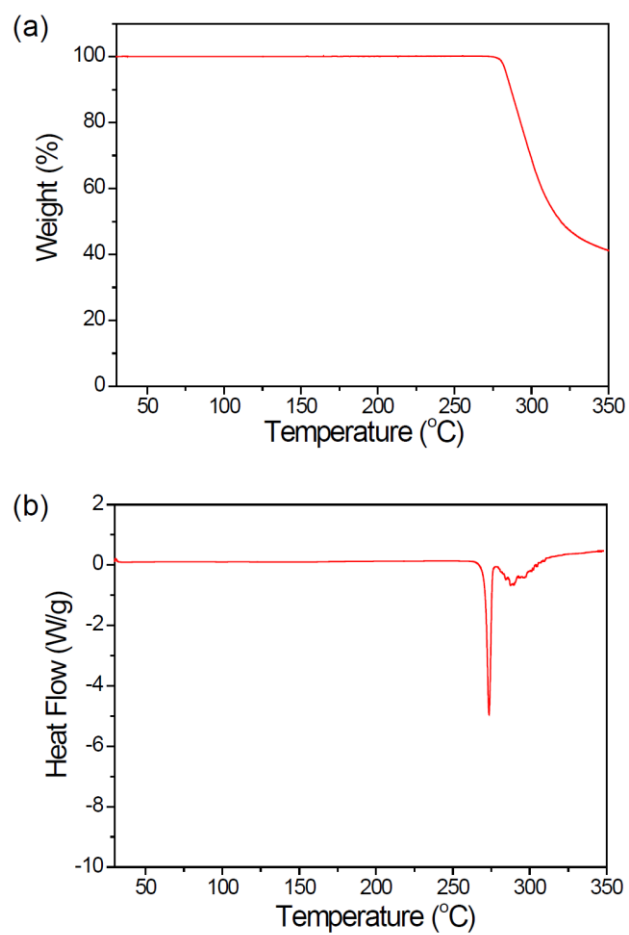


Figure S1. Thermal gravimetric analysis (TGA) and differential scanning calorimetry (DSC) thermodiagram of HMQ-TMS crystals (scanning rate 10 K/min).

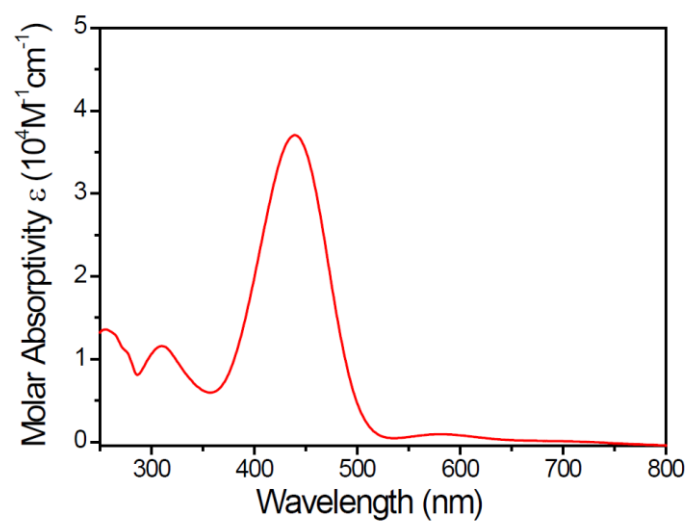


Figure S2. Absorption spectra of HMQ-TMS in methanol solution: $\lambda_{\text{max}} = 439 \text{ nm}$.

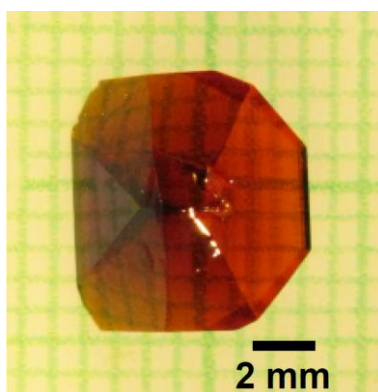


Figure S3. Photograph of a large-size HMQ-TMS crystal, grown by slow cooling method with a seed at a saturation temperature of $40 \text{ }^\circ\text{C}$ in methanol.

Humidity resistance measurement

HMQ-TMS powder (0.1 g) was dissolved in water-containing solvent mixture, 18-mL methanol and 2-mL water. HMQ-TMS crystals were grown by slow evaporation method in an oven at a constant temperature of 40°C. The solvent evaporated until the solution of about 4 mL was remained, and the crystals were then obtained by filtration.

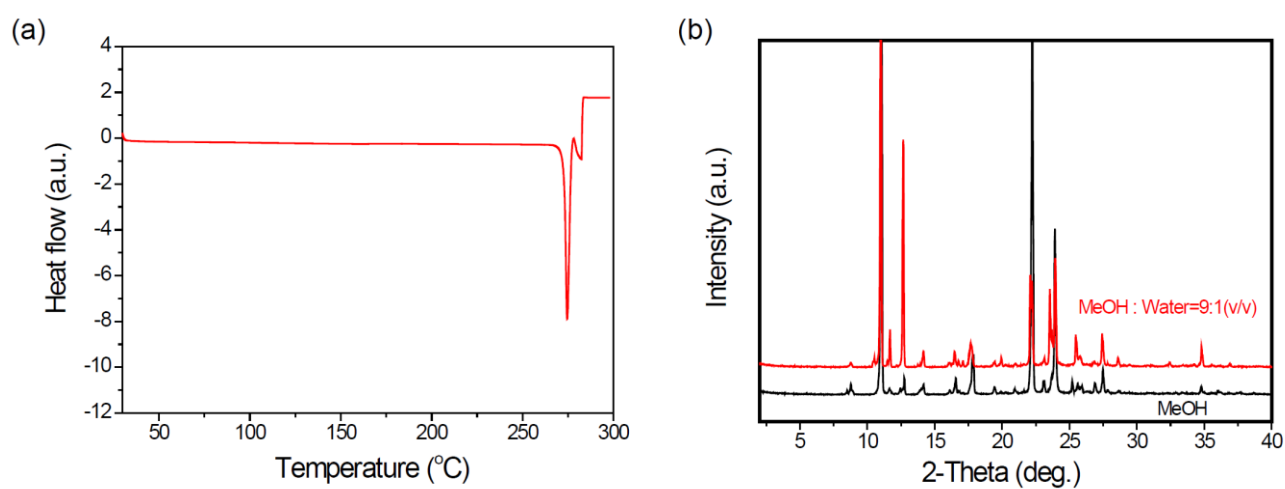


Figure S4. (a) DSC thermodiagram and (b) powder X-ray diffraction pattern of HMQ-TMS crystals grown in water-containing solvent mixture.

Atomic force microscopy

All the atomic force microscopy (AFM) images were recorded in non-contact mode on a XE-100 AFM system (PSIA, Inc., South Korea) with conventional Si cantilevers (M2N, Inc., Korea, spring constant 40N/m, and model TETRA 15 (50)) in ambient condition. The Si cantilevers were vibrated with a resonance frequency of approximately 310 kHz.

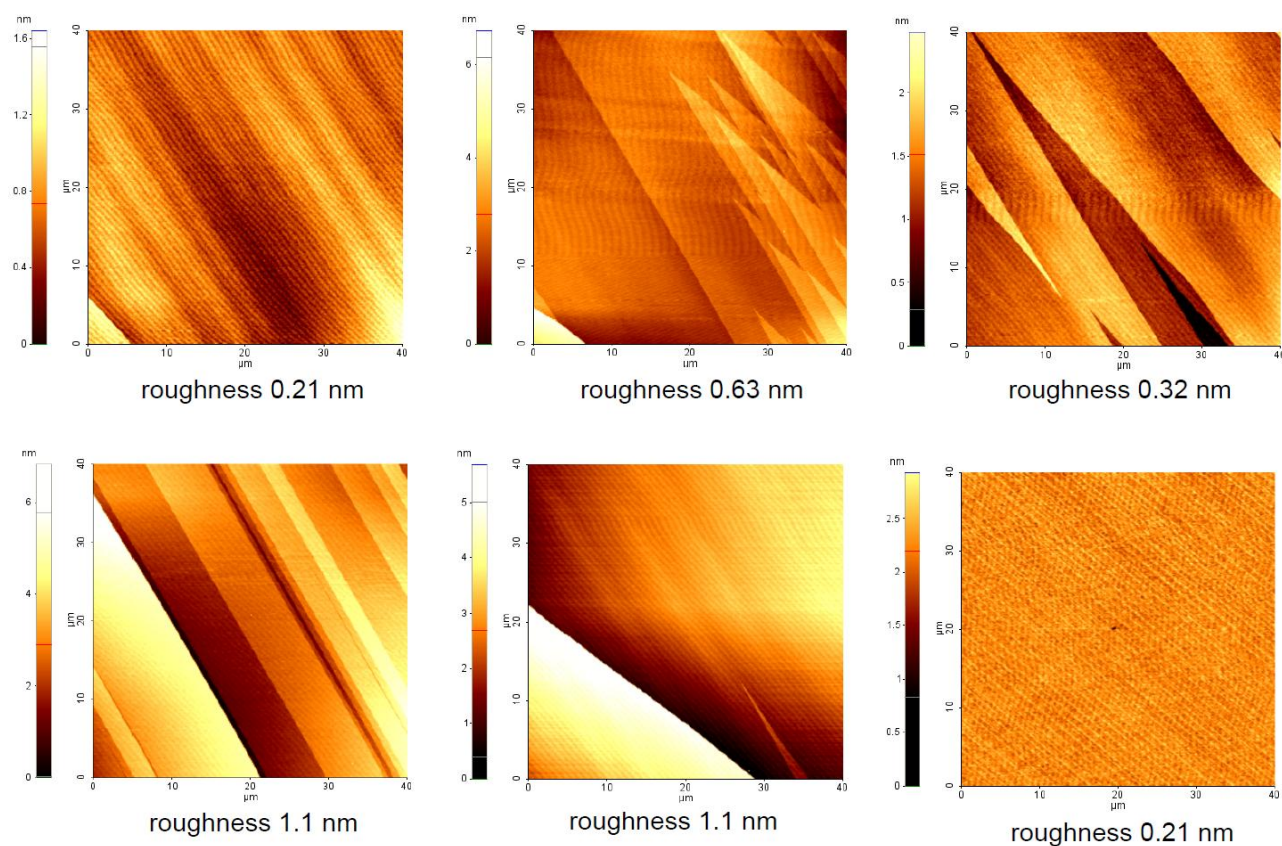


Figure S5. AFM images in the cleaving surface of HMQ-TMS crystals in Figure 2c (area: 40×40 μm²). The roughness of cleaving surface with area of 40×40 μm² in various positions is less than 1.3 nm.

THz wave generation experiments

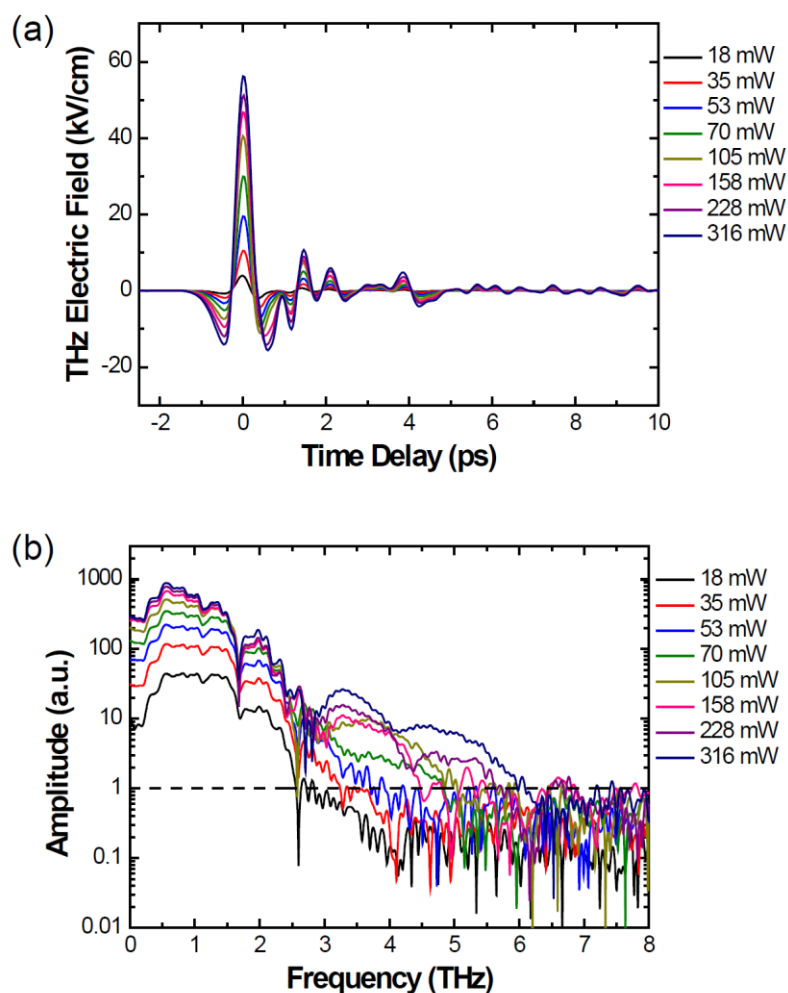


Figure S6. THz wave generation in 0.22-mm-thick HMQ-TMS crystal using different incident average pump powers P_{pump} with a beam diameter of $D = 3.0$ mm: (a) Selected time-domain THz electric field $E_{\text{THz}}(t)$ traces and (b) the corresponding frequency spectra of $E_{\text{THz}}(\nu)$ in logarithm scale depicted in Figure 3f.

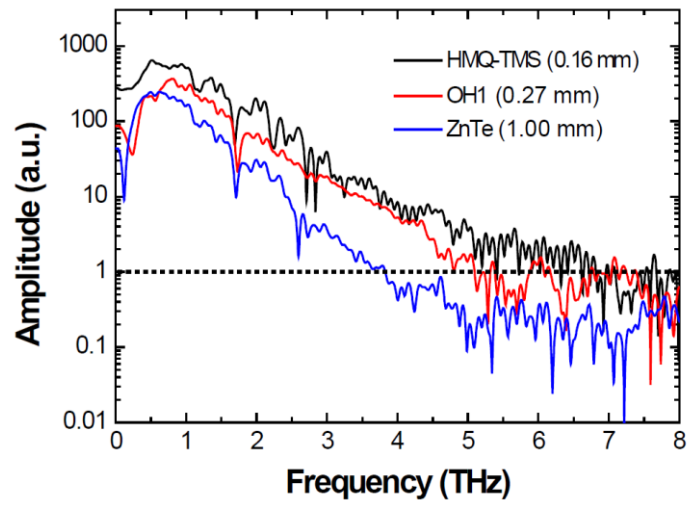


Figure S7. THz wave generation in 0.16-mm-thick HMQ-TMS, 0.27-mm-thick OH1 and 1.0-mm-thick ZnTe crystals ($P_{\text{pump}} = 158 \text{ mW}$, $D = 3.0 \text{ mm}$): frequency spectra of $E_{\text{THz}}(\nu)$ in logarithm scale depicted in Figure 4b.